Journal of Alloys and Compounds 588 (2014) 96–102

Contents lists available at ScienceDirect

Journal of Alloys and Compounds

journal homepage: www.elsevier.com/locate/jalcom

Phase stability, elastic and electronic properties of Cu–Zr binary system intermetallic compounds: A first-principles study

Jinglian Du [a], Bin Wen [a,*], Roderick Melnik [b], Yoshiyuki Kawazoe [c,d]

[a] State Key Laboratory of Metastable Materials Science and Technology, Yanshan University, Qinhuangdao 066004, China
[b] M²NeT Lab, Wilfrid Laurier University, Waterloo,75 University Ave. West, Ontario N2L 3C5, Canada
[c] New Industry Creation Hatchery Center, Tohoku University, 6-6-4 Aramaki-aza-Aoba, Aoba-ku, Sendai 980-8579, Japan
[d] Institute of Thermophysics, Siberian Branch of the Russian Academy of Sciences, 1 Lavyrentyev Avenue, Novosibirsk 630090, Russia

ARTICLE INFO

Article history:
Received 28 July 2013
Received in revised form 22 September 2013
Accepted 4 November 2013
Available online 16 November 2013

Keywords:
Cu–Zr intermetallic compounds
Phase stability
Elastic properties
Electronic band structure
First-principles study

ABSTRACT

First-principle calculations have been performed to investigate the structural, mechanical, thermodynamic and electronic properties of eight binary Cu–Zr intermetallic compounds. The results indicated that with increasing Zr concentration, the mass density decreases monotonously. All Cu–Zr intermetallic compounds considered here are mechanically stable structures, and they are ductile materials. Among the eight binary Cu–Zr intermetallic compounds, CuZr is the most ductile phase. Furthermore, the heats of formation of the Cu–Zr intermetallic compounds are negative. Furthermore, $CuZr_2$ is a semiconductor with indirect band gap of 0.227 eV, while the other seven Cu–Zr intermetallic compounds considered here are conductors.

1. Introduction

Since its high glass forming ability, Cu–Zr binary alloys have become a typical binary system to study the amorphous metals [1–5]. Meanwhile, both Cu–Zr amorphous metals and their intermetallics counterparts have outstanding properties (e.g. ultrahigh-yield strengths, large elastic strain limits, high hardness, corrosion resistance and low fracture toughness), and hence they have extensive applications in structural, chemical and magnetic fields [6–8]. Therefore, Cu–Zr binary alloys have drawn considerable scientific and technological attention.

For binary or ternary Cu–Zr system amorphous metals, their glass forming ablility is related with the thermodynamic stability of corresponding equilibrium intermetallic compounds [9–12], and the mechanical properties of Cu–Zr amorphous metals are also closely associated with mechanical properties of their intermetallics counterparts [13–24]. Hence many researchers have devoted themselves to the design of Cu–Zr amorphous metals on the basis of thermodynamic and mechanical properties of their corresponding equilibrium intermetallic compounds [25–34]. Therefore, the phase diagram of Cu–Zr binary system, as well as the thermodynamic and mechanical properties of Cu–Zr binary intermetallic compounds turn into keypoints in the studies of Cu–Zr binary alloys. As a result, many theoretical and experimental works have been performed to determine the Cu–Zr binary phase diagram, the thermodynamic and mechanical properties of Cu–Zr binary intermetallic compounds [35–54].

According to the Cu–Zr binary phase diagram [35–46], there are eight intermetallic compounds in the Cu–Zr binary alloy system, namely $CuZr_2$, CuZr, $Cu_{10}Zr_7$, Cu_8Zr_3, $Cu_{51}Zr_{14}$, Cu_5Zr, Cu_2Zr, and Cu_5Zr_8. Among them, the CuZr phase has been extensively investigated. For example, various aspects including heats of formation, structural, electronic and elastic properties of CuZr phase have been explored intensively [13,14,52,77]. However, the mechanism of shape memory effect for CuZr phase is still unclear; in order to uncover this mechanism, a theoretical study of intrinsic ductility and brittleness of CuZr is needed. As for the other Cu–Zr intermetallic compounds, a number of existing studies have mainly been focused on their thermodynamic properties and phase stability. For example, in 2003, Zaitsev et al. have performed a complete experimental thermodynamic description of Cu–Zr intermetallic compounds and obtained the evidence of the existence of Cu_2Zr and Cu_5Zr_8 phase [46]. In 2007, Ghosh have studied the cohesive properties of Cu–Zr intermetallic compounds by first principles calculations and found that Cu_5Zr, Cu_8Zr_3, $Cu_{10}Zr_7$ and $CuZr_2$ phases are stable phases at 0 K, while $Cu_{51}Zr_{14}$ is metastable at 0 K [52]. In 2008, Yamaguchi et al. have also experimentally measured the standard enthalpies of formation of Cu_9Zr_2, $Cu_{51}Zr_{14}$,

* Corresponding author. Tel.: +86 335 8568761.
E-mail address: wenbin@ysu.edu.cn (B. Wen).

0925-8388/$ - see front matter © 2013 Elsevier B.V. All rights reserved.
http://dx.doi.org/10.1016/j.jallcom.2013.11.018

Cu_8Zr_3, $Cu_{10}Zr_7$ and $CuZr_2$ at 298.15 K [42]. In 2010, Zhou et al. have investigated the phase stability of Cu–Zr intermetallic compounds by both first principles calculations and experimental methods, and concluded that $Cu_{51}Zr_{14}$ and $CuZr_2$ are stable phases, while Cu_5Zr, $Cu_{10}Zr_7$, CuZr and Cu_5Zr_8 are metastable phases at 0 K [53]. In view of all the above, we can see that these previously reported results are incongruent, so further study along this direction is still required to understand the phase stability of Cu–Zr intermetallic compounds. Moreover, although a significant progress has been made on the studies of Cu–Zr binary alloys, as far as we know, stoichiometry-dependent structural, mechanical, thermodynamic and electronic properties remain poorly characterized and understood. To fill this gap, a systematic first-principles calculations are performed to investigate the structural, mechanical, thermodynamic and electronic properties of Cu–Zr intermetallic compounds.

2. Computational methods

In this work, the crystallographic data of the eight binary Cu–Zr intermetallic compounds (i.e. $CuZr_2$, CuZr, $Cu_{10}Zr_7$, Cu_8Zr_3, $Cu_{51}Zr_{14}$, Cu_5Zr, Cu_2Zr and Cu_5Zr_8) are taken from Refs. [52,58], and they are listed in Table 1. The first principles calculations have been performed within the framework of electronic density functional theory (DFT), as implemented in the Vienne Ab initio Simulation Package (VASP) [55]. The exchange and correlation interaction was described by the generalized gradient approxiamation (GGA) with the Perdew–Wang (PW91) parameterization [56]. The interactions between ions and valence electrons were modeled by the projector-augmented wave (PAW) method [57]. The pseudopotentials employed in this work explicitly treat eleven valence electrons for copper (Cu $3d^{10}4p^1$) and four for zirconium (Zr $4d^3 4s^1$). A plain wave cutoff energy for 320 eV has been used. Brillouin zone integrations were performed by using a Monkhorst–Pack k-point mesh, and the k-point mesh of each cell has been sampled by $4 \times 4 \times 4$, $8 \times 8 \times 2$, $3 \times 3 \times 2$, $8 \times 8 \times 8$, $5 \times 3 \times 5$, $1 \times 3 \times 8$, $3 \times 3 \times 4$ and $3 \times 3 \times 2$ grids for Cu_5Zr, $CuZr_2$, Cu_8Zr_3, CuZr, Cu_2Zr, Cu_5Zr_8, $Cu_{51}Zr_{14}$ and $Cu_{10}Zr_7$, respectively. The total energy was converged numerically to 5×10^{-7} eV/atom with respect to electronic, inonic and unit cell degrees of freedom.

To verify computational accuracy, benchmark calculations have been performed for the CuZr intermetallic compound. The lattice parameters after optimization for bulk CuZr alloy phase agree well with the available experimental [58] and previously reported theoretical values [52], which confirmed that the computational scheme used in this work is reliable.

3. Results and discussion

3.1. The structural properties

The lattice parameters and internal coordinates of the eight Cu–Zr intermetallic compounds have been optimized by using density functional theory calculations, and the optimized lattice parameters and the corresponding mass densities, together with the available experimental and theoretical values are listed in Table 1. As shown in Table 1, the calculated values are in good agreement with the available experimental and other theoretical data. Although the Vegard's law [59] indicates that a linear relation exists between the lattice parameters and elements concentration, the intermetallic compounds in the Cu–Zr binary alloy system have been found that do not obey this law. This may be attributed to the fact that the Vegard's empirical rule is considered to be valid for the same type crystal symmetry, while the eight intermetallic compounds studied here do not possess the same symmetry [60].

The relationships between the mass density and Zr concentration of Cu–Zr intermetallic compounds are depicted in Fig. 1. As we know, the mass density of pure copper (8783.8 kg/m^3) is larger than that of pure zirconium (6478.7 kg/m^3). Thus, with the increasing Zr-concentration, the mass densities of Cu–Zr intermetallic compounds decrease almost linearly. Further, the mass density ρ (kg/m^3) of Cu–Zr intermetallic compounds decreases approximately in a linear manner (i. e. $\rho = 8559.84\ 22.95c$) with the increasing Zr concentration c (at.%).

3.2. Mechanical stability and elastic properties

To investigate the mechanical stability and relevant materials properties, we have calculated the single-crystal elastic constants of the related phases (i.e. Cu–Zr intermetallic compounds as well as pure copper and zirconium) in their stable ground state structures. In this work, the single-crystal elastic constants were obtained by computing the total energy density as a function of suitable strains [61,62]. Based on the crystal system and various imposed deformations, the quadratic coefficient of the total energy density versus strain corresponds to a linear combination of particular elastic constants [63,64]. In this study, the total energies of the

Table 1
Theoretical and experimental crystallographic data and mass density for the Cu–Zr binary system intermetallic compounds.

Phase	Space group	Prototype	Unit cell lattice parameters (nm)			Mass density (kg/m^3)	Reference
Cu	$Fm\bar{3}m$	Cu	a = 0.3636			8783.8	This work
			a = 0.3608			8940.0	[58]
Cu_5Zr	$F\bar{4}3m$	$AuBe_5$	a = 0.6916			8211.9	This work
			a = 0.6870				[58]
$Cu_{51}Zr_{14}$	$P6/m$	$Ag_{51}Gd_{14}$	a = 1.1454		c = 0.8260	7993.4	This work
			a = 1.1244		c = 0.8282		[58]
Cu_8Zr_3	Pnma	Cu_8Hf_3	a = 0.7910	b = 0.8216	c = 1.0032	7967.2	This work
			a = 0.7869	b = 0.8155	c = 0.9985		[58]
Cu_2Zr	Amm2	Au_2V	a = 0.4685	b = 0.8576	c = 0.4685	7704.2	This work
			a = 0.4686	b = 0.8498	c = 0.4686		[52]
$Cu_{10}Zr_7$	Aba2	$Ni_{10}Zr_7$	a = 0.9404	b = 0.9364	c = 1.2756	7533.9	This work
			a = 0.9347	b = 0.9313	c = 1.2675	7673.0	[58]
CuZr	$Pm\bar{3}m$	CsCl	a = 0.3280			7282.5	This work
			a = 0.3262				[58]
Cu_5Zr_8	Pbam	$Al_2Bi_6Ca_5$	a = 1.9865	b = 0.7702	c = 0.3209	7083.1	This work
			a = 1.9738	b = 0.7688	c = 0.3184		[52]
$CuZr_2$	$I4/mmm$	$MoSi_2$	a = 0.3236	b = 1.1204		6963.1	This work
			a = 0.3220	b = 1.1183			[58]
Zr	$P6_3/mmc$	Zr	a = 0.3230		c = 0.5175	6478.7	This work
			a = 0.3232		c = 0.5148	6556.0	[58]

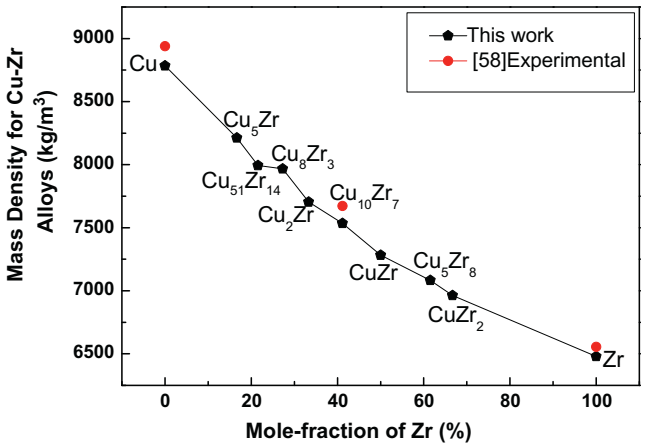

Fig. 1. Theoretical mass density compared to experimental values for the Cu–Zr binary system intermetallic compounds.

relevant phases have been calculated by imposing appropriate strains up to ± 1.25% at 0.25% interval.

According to the above methods, the single-crystal elastic constants of the eight Cu–Zr intermetallic compounds as well as pure copper and zirconium have been calculated and summarized in Table 2, together with the previous experimental and theoretical values. As shown in Table 2, for CuZr, pure copper and zirconium, our calculated single-crystal elastic constants are in good agreement with the available experimental and previous theoretical values [52,54,65,66,77,78]. To the best of our knowledge, however, there are no available experimental and theoretical elastic constants for other seven Cu–Zr intermetallic compounds. Thus, our calculated results of single-crystal elastic constants for $CuZr_5$, $Cu_{51}Zr_{14}$, Cu_8Zr_3, Cu_2Zr, $Cu_{10}Zr_7$, Cu_5Zr_8 and $CuZr_2$ intermetallic compounds will provide useful data for comparision with future experimental measurements as well as theoretical investigations.

As an important part of theoretical research on phase stability, the mechanical stability of crystal can be acquired from the knowledge of its single-crystal elastic constants. Combining single-crystal elastic constants with the mechanical stability evaluated criterion, we analysed the mechanical stability of the binary Cu–Zr intermetallic compounds. In terms of the eight Cu–Zr intermetallic compounds considered in this study, CuZr and Cu_5Zr belong to the cubic crystal system, $CuZr_2$ belongs to the tetragonal crystal system, $Cu_{51}Zr_{14}$ belongs to the hexagonal crystal system, while Cu_2Zr, Cu_5Zr_8, Cu_8Zr_3 and $Cu_{10}Zr_7$ belong to the orthorhombic crystal system.

The requirements of mechanical stability for the cubic crystal system structures [67] are given by the following formula:

$$C_{11} > 0, \quad C_{44} > 0, \quad C_{11} > |C_{12}|, \quad C_{11} + 2C_{12} > 0. \tag{1}$$

As shown in Table 2, the elastic constants of the cubic crystal system structures CuZr and Cu5Zr satisfy the above mechanical stability criteria, confirming that CuZr and Cu5Zr are mechanically stable phases.

For tetragonal crystal system structures, the mechanical stability criteria [67] are given by the following formula:

$$C_{11} > 0, \quad C_{33} > 0, \quad C_{44} > 0, \quad C_{66} > 0, \quad C_{11} - C_{12} > 0,$$
$$C_{11} + C_{33} - 2C_{13} > 0, \quad 2(C_{11} + C_{12}) + C_{33} + 4C_{13} > 0. \tag{2}$$

All the values of elastic constants for tetragonal crystal system structure $CuZr_2$ satisfy the mechanical stability restrictions in Eq. (2), demonstrating that $CuZr_2$ is mechanically stable.

The restrictions of mechanical stability for hexagonal crystal system structures [67] are given by the following formula:

$$C_{44} > 0, \quad C_{11} > |C_{12}|, \quad (C_{11} + 2C_{12})C_{33} > 2C_{13}^2. \tag{3}$$

As can be seen, the single-crystal elastic constants for hexagonal crystal system structure $Cu_{51}Zr_{14}$ satisfy the mechanical stability restrictions in Eq. (3), indicating that $Cu_{51}Zr_{14}$ is mechanically stable.

As for orthorhombic crystal system structures, the mechanical stability criteria [67] are given by the following formula:

$$C_{11} > 0, \quad C_{22} > 0, \quad C_{33} > 0, \quad C_{44} > 0, \quad C_{55} > 0, \quad C_{66} > 0,$$
$$C_{11} + C_{22} + C_{33} + 2(C_{12} + C_{13} + C_{23}) > 0, \quad C_{11} + C_{22} - 2C_{12} > 0,$$
$$C_{11} + C_{33} - 2C_{13} > 0, \quad C_{22} + C_{33} - 2C_{23} > 0. \tag{4}$$

Based on the single-crystal elastic constants presented in Table 2, all the orthorhombic crystal system structures of Cu-Zr intermetallic compounds satisfy the mechanical stability requirements in Eq. (4), implying that Cu_2Zr, Cu_8Zr_3, Cu_5Zr_8 and $Cu_{10}Zr_7$ are mechanically stable.

According to the above analysis, all the eight Cu-Zr intermetallic compounds considered in this study (i.e. Cu_5Zr, Cu_2Zr, $Cu_{10}Zr_7$, CuZr, $Cu_{51}Zr_{14}$, Cu_8Zr_3, $CuZr_2$ and Cu_5Zr_8) are mechanically stable.

Table 2
Calculated single-crystal elastic constants compared to experimental and other theoretical values for the Cu–Zr binary system intermetallic compounds.

Phase	Single-crystal elastic constants (GPa)					Reference
Cu	C_{11} = 179	C_{12} = 134	C_{44} = 73			This work
	C_{11} = 176	C_{12} = 125	C_{44} = 81			[64]
	C_{11} = 171	C_{12} = 123	C_{44} = 72			[52]
Cu_5Zr	C_{11} = 226	C_{12} = 94	C_{44} = 73			This work
$Cu_{51}Zr_{14}$	C_{11} = 189	C_{12} = 90	C_{13} = 86	C_{33} = 193	C_{44} = 43	This work
Cu_8Zr_3	C_{11} = 202	C_{12} = 105	C_{13} = 94	C_{22} = 206	C_{23} = 98	This work
	C_{33} = 200	C_{44} = 58	C_{55} = 57	C_{66} = 64		
Cu_2Zr	C_{11} = 218	C_{12} = 99	C_{13} = 49	C_{22} = 191	C_{23} = 100	This work
	C_{33} = 216	C_{44} = 57	C_{55} = 10	C_{66} = 59		
$Cu_{10}Zr_7$	C_{11} = 190	C_{12} = 88	C_{13} = 102	C_{22} = 185	C_{23} = 105	This work
	C_{33} = 167	C_{44} = 63	C_{55} = 63	C_{66} = 47		
CuZr	C_{11} = 140	C_{12} = 112	C_{44} = 43			This work
	C_{11} = 138	C_{12} = 112	C_{44} = 45			[52]
	C_{11} = 138	C_{12} = 113	C_{44} = 44			[54]
Cu_5Zr_8	C_{11} = 146	C_{12} = 83	C_{13} = 92	C_{22} = 162	C_{23} = 91	This work
	C_{33} = 145	C_{44} = 46	C_{55} = 43	C_{66} = 40		
$CuZr_2$	C_{11} = 169	C_{12} = 74	C_{13} = 91	C_{33} = 150	C_{44} = 66	This work
	C_{66} = 32					
Zr	C_{11} = 163	C_{12} = 53	C_{13} = 69	C_{33} = 179	C_{44} = 20	This work
	C_{11} = 138	C_{12} = 72	C_{13} = 71	C_{33} = 160	C_{44} = 23	[52]
	C_{11} = 156	C_{12} = 65	C_{13} = 76	C_{33} = 182	C_{44} = 25	[76]
	C_{11} = 155	C_{12} = 67	C_{13} = 65	C_{33} = 173	C_{44} = 36	[64]

To better understand the mechanical properties of binary Cu–Zr intermetallic compounds, the bulk modulus (K), shear modulus (G), Young's modulus (E) and Poisson's ratio (u) for polycrystalline materials have been obtained from single-crystal elastic constants by using Voigt, Reuss and Hill (VRH) approximations [68,69]. The related approximation formulas are given as follows:

$$\begin{aligned} K_{VRH} &= K^* = (K_v + K_R)/2 \\ G_{VRH} &= G^* = (G_V + V_R)/2 \\ E_{VRH} &= 9K_{VRH}G_{VRH}/G_{VRH} + 3K_{VRH} \end{aligned} \quad (5)$$

where

$$\begin{aligned} K_{V,R} &= (C11 + 2C12)/3 \\ G_V &= (C_{11} - C_{12} + 3C_{44})/5 \\ G_R &= 5(C_{11} - C_{12})C_{44}/[4C_{44} + 3(C_{11} - C_{12})] \end{aligned} \quad (6)$$

The computed results are summarized in Table 3. The relationship between bulk modulus and concentration of Zr has been depicted in Fig. 2, from which we can see that the bulk modulus of Cu–Zr intermetallic compounds decreases with increasing Zr concentration (at.%). This variation trend is analogous to that of the mass density, confirming the fact that the bulk modulus is closely related with the mass density [77]. Similarly, Fig. 3 presents the correlation for the shear modulus (G) and Young's modulus (E) against the concentration of Zr. As shown in Fig. 3, Cu_5Zr has the largest G and E values of 70 GPa and 180 GPa, while CuZr has the smallest G and E values of 28 GPa and 78 GPa. It is reported that the hardness of a material is associated with its shear modulus and Young's modulus. Although the accurate relationship between hardness and elastic modulus is still undetermined, a large elastic modulus represents high hardness [70–72]. Therefore, among the eight Cu–Zr intermetallic compounds considered here, Cu_5Zr has the highest hardness, while the hardness of CuZr is the lowest.

Table 3
Polycrystalline shear modulus (G), bulk modulus (K), Young's modulus (E), Poisson's ratio (u), G/K ratio and energy band gaps (E_g) for the Cu–Zr binary system intermetallic compounds, deduced by single-crystal elastic constants and Voigt, Reuss and Hill (VRH) approximations.

Phase	G (GPa)	K (GPa)	E (GPa)	u	G/K	E_g (eV)
Cu_5Zr	70	138	180	0.283	0.5072	0
$Cu_{51}Zr_{14}$	47	122	126	0.328	0.3890	0
Cu_8Zr_3	56	133	148	0.315	0.4220	0
Cu_2Zr	40	124	108	0.355	0.3210	0
$Cu_{10}Zr_7$	49	126	131	0.326	0.3940	0
CuZr	28	121	78	0.393	0.2298	0
Cu_5Zr_8	37	109	101	0.347	0.3419	0
$CuZr_2$	46	111	121	0.319	0.4128	0.227

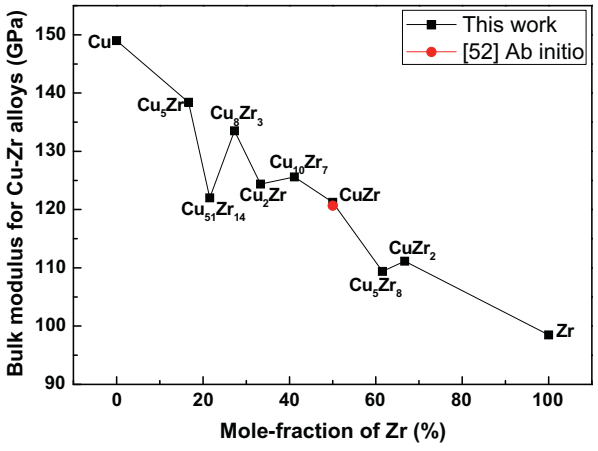

Fig. 2. Calculated bulk modulus (B) versus concentration of Zr for the Cu–Zr binary system intermetallic compounds.

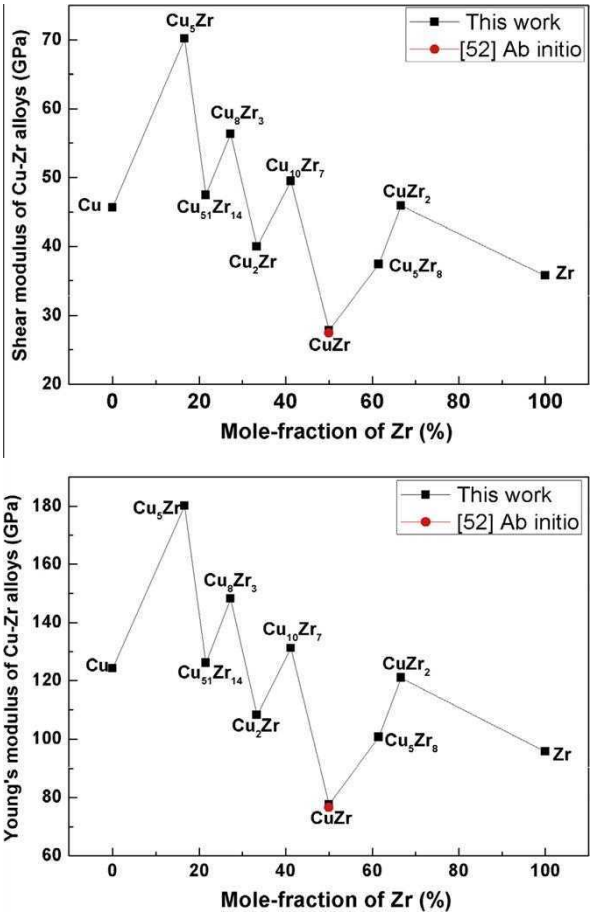

Fig. 3. Calculated shear modulus (G) and Young's modulus (E) versus concentration of Zr for the Cu–Zr binary system intermetallic compounds.

Based on the elastic modulus, the ratio of shear modulus to bulk modulus (G/K), which can be used to estimate the brittleness and toughness of intermetallic compounds [73], is being calculated. The critical value of the G/K ratio is 0.57, i. e. the intermetallics for which G/K ratio is larger than 0.57 are considered brittle, otherwise are ductile [73]; and this criterion has been proved reasonable for many intermetallic compounds [74–76]. Generally speaking, the lower ratio of G/K, the more ductile the materials would be. To analyze this further, the G/K ratios of Cu-Zr intermetallic compounds have been computed and presented in Table 3. As shown in Table 3, the G/K ratio for Cu_5Zr, Cu_2Zr, $Cu_{51}Zr_{14}$, $Cu_{10}Zr_7$, Cu_8Zr_3, CuZr, Cu_5Zr_8 and $CuZr_2$ are 0.507, 0.321, 0.389, 0.394, 0.422, 0.230, 0.342 and 0.413, respectively. All these values are lower than 0.57, implying that the eight Cu–Zr intermetallic compounds considered here are ductile. Particularly, the CuZr phase is the most ductile phase among these Cu–Zr intermetallic compounds, this is inconsistent with previous studies [23,77,78]. In addition, the large Poisson's ratio of 0.393 for CuZr phase also indicated that CuZr is the most ductile phase among these intermetallic compounds. This is consistent with above G/K discussions since Poission's ratio (u) can be expressed in terms of G/K for isotropic materials [79]:

$$u = [3(K/G) - 2]/[6(K/G) + 2] \quad (7)$$

It is reported that the elastic properties of amorphous metals can be estimated from their corresponding intermetallic compounds counterparts. For example, the bulk modulus of amorphous

alloys is about 6% smaller than the crystalline alloys with similar composition, while both the shear modulus and Young's modulus of metallic glasses are about 30% smaller than the corresponding values for crystals [78,80]. Thus, our investigations on the elastic properties of Cu–Zr intermetallic compounds will provide useful information for researchers to further study the corresponding properties of Cu–Zr amorphous metals.

3.3. Thermodynamic stability

In order to study the thermodynamic properties of Cu–Zr intermetallic compounds, we have computed the ground state total energies of the eight Cu–Zr intermetallic compounds as well as pure copper and zirconium. For a given Cu–Zr intermetallic compound Cu_aZr_b, the heats of formation is defined as the differences between the total energy of Cu_aZr_b and the linear combination of the pure copper and zirconium stable state energies. Subsequently, the heats of formation for Cu–Zr intermetallic compounds can be expressed by the following formula:

$$E_{form}^{Cu_aZr_b} = \left[E_{total}^{Cu_aZr_b} - \left(aE_{solid}^{Cu} + bE_{solid}^{Zr}\right)\right]/(a+b). \quad (8)$$

In Eq. (8), $E_{form}^{Cu_aZr_b}$ refers to the heats of formation for Cu_aZr_b intermetallic compound, $E_{total}^{Cu_aZr_b}$ is the total energy of the Cu_aZr_b primate cell containing "a"Cu atoms and "b"Zr atoms with their stable ground state structures, E_{solid}^{Cu} is the total energy of one Cu atom in face-centered cubic structure with its equilibrium lattice parameters and E_{solid}^{Zr} is the total energy of one Zr atom in hexagonal close-packed structure with its corresponding equilibrium lattice parameters.

According to Eq. (5), the heats of formation for the eight Cu–Zr intermetallic compounds considered here are summarized in Table 4 and also plotted in Fig. 4, together with available experimental and other theoretical values found in the literature. It should be noted that for Fig. 4, we have taken the ground state convex hull defined by Cu_5Zr, Cu_8Zr_3, $Cu_{10}Zr_7$ and $CuZr_2$ phases in our investigations, considering that the four intermetallic compounds are known to be stable phases at 0 K [46,49,52].

Based on the calculated heats of formation, the thermodynamic stability of Cu-Zr intermetallic compounds has been analysed. As shown in Fig. 4, Cu_5Zr, Cu_8Zr_3, $Cu_{10}Zr_7$ and $CuZr_2$ phases are stable phases, and these results are in agreement with previously reported results [49,52,81,82]. Our calculated heats of formation for $Cu_{51}Zr_{14}$, Cu_2Zr, Cu_5Zr_8, CuZr phases are -9.515, -11.628, -5.34 and -6.061 kJ/mol atoms, and they lie 4.32, 4.638, 8.013, and 8.854 kJ/mol atoms above the ground state convex hull, respectively. These results correspond to the experimental fact that the CuZr, Cu_5Zr_8 and Cu_2Zr intermetallic compounds can decompose into the other stabler phases (i. e. $CuZr \rightarrow Cu_{10}Zr_7 + Cu_5Zr_8$, $Cu_5Zr_8 \rightarrow Cu_{10}Zr_7 + CuZr_2$ and $Cu_2Zr \rightarrow Cu_8Zr_3 + Cu_{10}Zr_7$) [37,38,40,43,46,49,51,52,83,84].

All heats of formation for the eight Cu–Zr intermetallic compounds considered here are negative, and the absolute heats of formation for Cu_5Zr, $Cu_{51}Zr_{14}$, Cu_8Zr_3, Cu_2Zr, $Cu_{10}Zr_7$, CuZr, Cu_5Zr_8 and $CuZr_2$ are 11.77, 9.5, 16.3, 11.6, 16.1, 6.1, 5.3 and 12.7 kJ/mol atoms, respectively. These values indicate that the chemical interaction between Cu and Zr is not so tight, but the negative heats of formations imply that these intermetallic compounds are thermodynamically stable phases (see Fig. 4).

3.4. . The electronic properties

In order to understand the electronic properties of the eight Cu–Zr binary system intermetallic compounds, the electronic energy band structures and the corresponding density of state have been calculated based on the corresponding optimized structures. The calculated results are summarized in Fig. 5. The electronic energy band structures represent the energy of high symmetry directions. The dotted line in Fig. 5 is the Fermi energy level defining as the highest occupied orbital in the valence band at 0 K. As the energy band structures and their corresponding density of states shown in Fig. 5, except for $CuZr_2$, the other seven Cu–Zr intermetallic compounds are conductors since the top of valence band and the bottom of conduction band are overlapped for Cu_5Zr, $Cu_{51}Zr_{14}$, $Cu_{10}Zr_7$, Cu_2Zr, Cu_8Zr_3, CuZr and Cu_5Zr_8. For $CuZr_2$, our calculated result indicates that it is a semiconductor with indirect band gap

Table 4
The heats of formation for the Cu–Zr binary system intermetallic compounds, calculated in this work and known from the literature.

Phase	Heats of formation (kJ/mol atoms)	Reference
Cu_5Zr	−11.770	This work
	−12.522	[52]
	−10.299	[49]CALPHAD
$Cu_{51}Zr_{14}$	−9.515	This work
	−8.640	[52]
	−14.07	[43]
	−12.967	[49]CALPHAD
	−11.290	[51] CALPHAD
Cu_8Zr_3	−16.307	This work
	−18.205	[52]
	−15.815	[48] CALPHAD
	−13.460	[49]CALPHAD
	−11.095	[51] CALPHAD
Cu_2Zr	−11.628	This work
	−14.442	[52]
$Cu_{10}Zr_7$	−16.107	This work
	−18.755	[52]
	−12.31	[43]
	−14.221	[49]CALPHAD
	−14.988	[51] CALPHAD
	−21.235	[48] CALPHAD
CuZr	−6.061	This work
	−12.714	[52]
	−9.05	[43]
	−10.052	[49]CALPHAD
	−9.479	[51] CALPHAD
	−24.012	[48] CALPHAD
$CuZr_2$	−12.665	This work
	−14.521	[52]
	−10.95	[43]
	−14.635	[49]CALPHAD
	−15.029	[51] CALPHAD
	−17.167	[48] CALPHAD
Cu_5Zr_8	−5.340	This work
	−7.382	[52]

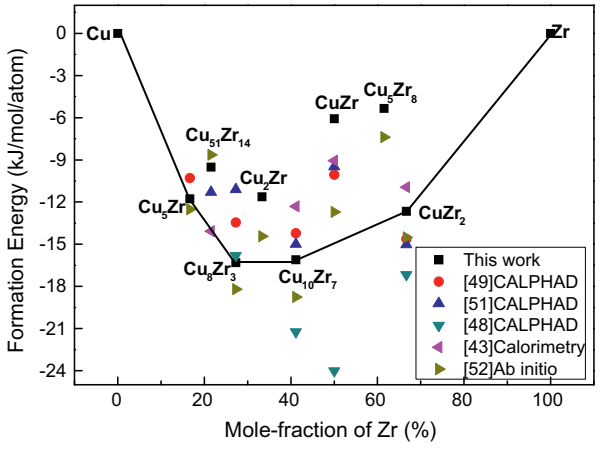

Fig. 4. Calculated heats of formation compared to experimental and other theoretical values for the Cu–Zr binary system intermetallic compounds.

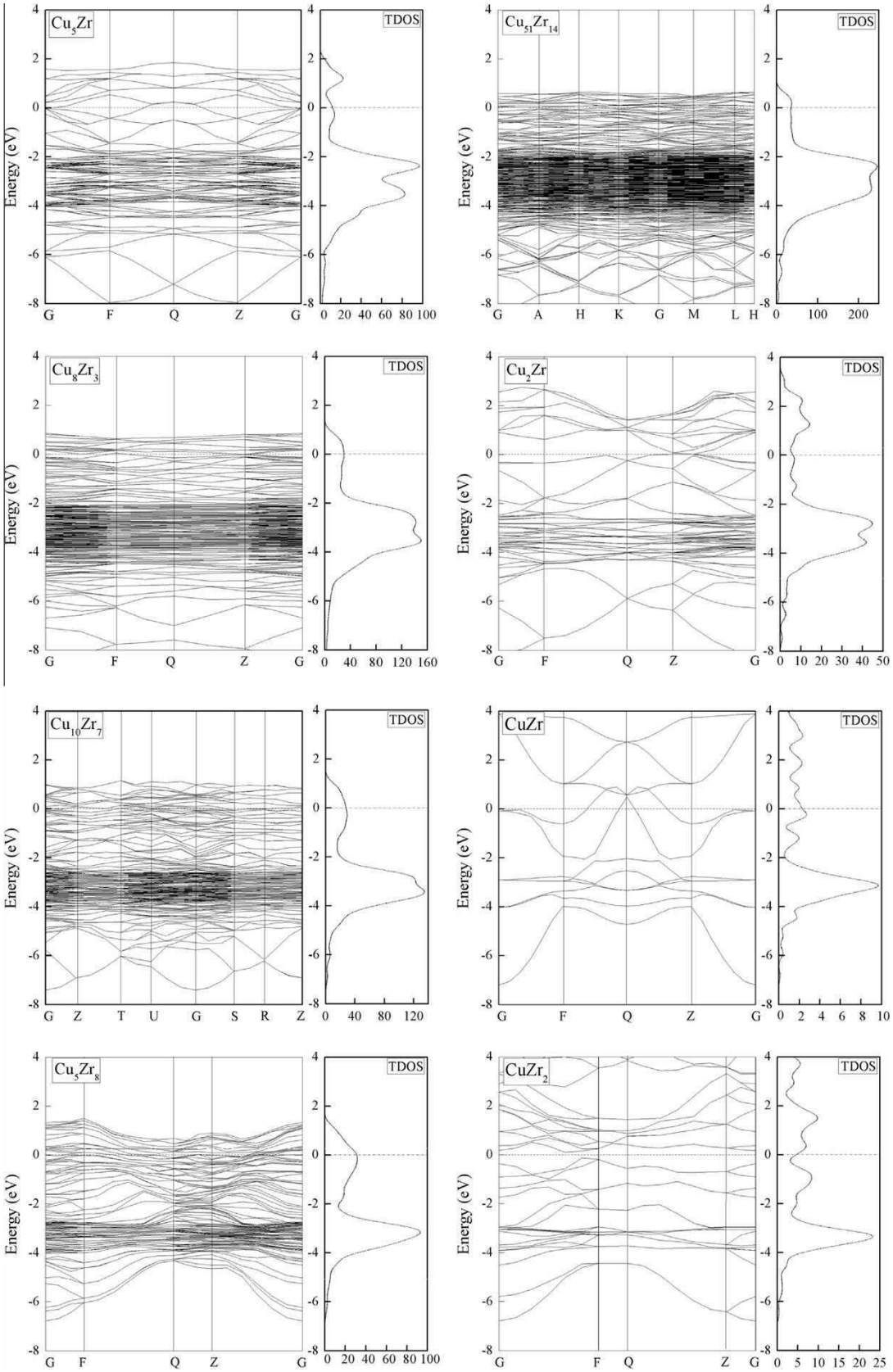

Fig. 5. Calculated electronic energy band structures and the corresponding density of states for the Cu–Zr binary system intermetallic compounds.

of 0.227 eV. In addition, it is known that the first-principles calculations usually underestimate the energy band gap of materials. Thus, the actual energy band gap for the $CuZr_2$ phase should be larger than this computed value.

4. Conclusion

In summary, we have performed first principles calculations on the phase stability of binary Cu–Zr intermetallic compounds (Cu_5Zr, $Cu_{51}Zr_{14}$, Cu_2Zr, $Cu_{10}Zr_7$, Cu_8Zr_3, CuZr, Cu_5Zr_8 and Cu_2Zr), with particular emphasis on the mechanical and thermodynamic stability. Meanwhile, the structural, elastic and electronic properties have also been investigated. The optimized lattice parameters are in good agreement with the available experimental and previous theoretical values. Moreover, the mass density of Cu–Zr intermetallic compounds decreases almost linearly with increasing Zr concentration.

Polycrystalline elastic moduli of Cu–Zr intermetallic compounds were deduced through single crystal elastic constants and Voigt, Russ and Hill (VRH) approximations. The ratio of shear modulus versus bulk modulus (G/K) indicated that the eight Cu–Zr intermetallic compounds are ductile materials and CuZr is the most ductile phase among these alloy phases. Furthermore, the bulk modulus (K) of Cu–Zr intermetallic compounds decreases with increasing Zr concentration. All the calculated heats of formation of the eight Cu–Zr intermetallic compounds are negative. In addition, the electronic energy band structure revealed that $CuZr_2$ is a semiconductor with indirect band gap of 0.227 eV, while the other seven Cu–Zr intermetallic compounds are conductors.

Acknowledgments

This work was supported by the National Natural Science Foundation of China (Grant No.'s 51121061 and 51131002), the Key Basic Research Program of Hebei Province of China (Grant No. 12965135D) and the Natural Science Foundation for Distinguished Young Scholars of Hebei Province of China (Grant No. E2013203265). R.M. acknowledges the support from the NSERC and CRC programs, Canada. The authors also would like to thank the staff of the Center for Computational Materials Science, Institute for Materials Research, Tohoku University for computer support. Y.K. is thankful to the CREST project headed by Prof. M. Kotani.

References

[1] Z. Altounian, Tu Guo-hua, J.O. Strom-Olsen, J. Appl. Phys. 53 (1982) 4755.
[2] T. Abe, M. Shimono, M. Ode, H. Onodera, J. Alloys Comp. 434 (2007) 152.
[3] J.C. Bendert, A.K. Gangopadhyay, N.A. Mauro, K.F. Kelton, Phys. Rev. Lett. 109 (2012) 185901.
[4] T.R. Chen, P.Y. Lee, J. Mar. Sci. Technol. 1 (1993) 59.
[5] D. Wang, Y. Li, B.B. Sun, M.L. Sui, K. Lu, E. Ma, Appl. Phys. Lett. 84 (2004) 4029.
[6] Y. Li, Q. Guo, J.A. Kalb, C.V. Thompson, Science 322 (2008) 1816.
[7] A. Inoue, N. Nishiyama, Mater. Res. Bull. 32 (2007) 651.
[8] A.L. Greer, E. Ma, Mater. Res. Bull. 32 (2007) 611.
[9] H. Tian, C. Zhang, L. Wang, J.J. Zhao, C. Dong, B. Wen, J. Appl. Phys. 109 (2011) 123520.
[10] I. Kaban, P. Jovari, V. Kokotin, O. Shuleshova, B. Beuneu, K. Saksl, N. Mattern, J. Echert, A.L. Greer, Acta Mater. 61 (2013) 2509.
[11] R.L. Freed, J.B. Vander, Sande, J. Non-Cryst. Solids 27 (1978) 9.
[12] K.H.J. Buschow, J. Appl. Phys. 52 (1981) 3319.
[13] N.Y. Koval, G.S. Firstov, A.V. Kotko, Scripta Metall. Mater. 27 (1992) 1611.
[14] D.C. Hofmann, Science 329 (2010) 1294.
[15] Z.D. Sha, B. Xu, L. Shen, A.H. Zhang, Y.P. Feng, Y. Li, J. Appl. Phys. 107 (2010) 063508.
[16] K.F. Kelton, Nat. Mater. 12 (2013) 473.
[17] C. Tang, P. Harrowell, Nat. Mater. 12 (2013) 507.
[18] K.H. Kang, K.W. Park, J.C. Lee, E. Fleury, B.J. Lee, Acta Mater. 59 (2011) 805.
[19] A. Peker, W.L. Johnson, Appl. Phys. Lett. 63 (1993) 2342.
[20] A.L. Greer, Science 267 (1995) 1947.
[21] C.T. Liu, J.O. Stiegler, Science 226 (1984) 636.
[22] R.A. Varin, M.B. Winnicka, Mater. Sci. Eng. A 137 (1990) 93.
[23] S. Pauly, J. Bednarcik, U. Kuhn, J. Eckert, Scripta Mater. 63 (2010) 336.
[24] K.H. Kim, J.P. Ahn, J.H. Lee, J.C. Lee, J. Mater. Res. 23 (2008) 1987.
[25] D.C. Hofmann, Nature 451 (2008) 1082.
[26] C.C. Hays, C.P. Kim, W.L. Johnson, Phys. Rev. Lett. 84 (2000) 2901.
[27] D.C. Hofmann, Proc. Natl. Acad. Sci. USA 105 (2008) 20136.
[28] S. Pauly, S. Gorantla, G. Wang, U. Kuhn, J. Eckert, Nat. Mater. 9 (2010) 473.
[29] D.V. Louzguine, H. Kato, A. Inoue, Appl. Phys. Lett. 84 (2004) 1088.
[30] C.J. Byrne, M. Eldrup, Science 321 (2008) 502.
[31] S. Pauly, Scripta Mater. 60 (2009) 431.
[32] S. Pauly, Appl. Phys. Lett. 95 (2009) 101906.
[33] G.Z. Ma, D. Chen, Z.H. Chen, J.W. Liu, W. Li, Mater. Sci-Poland 28 (2010) 595.
[34] G. Duan, K.D. Blauwe, M.L. Lind, J. P Schramm, W.L. Johnson, Scripta Mater. 58 (2008) 159.
[35] J.M Vitek, Z. Metallkd. 67 (1976) 559.
[36] A.F. Marshall, R.G. Walmsley, D.A. Stevenson, Mater. Sic. Eng. 63 (1984) 215.
[37] E. Kneller, Y. Khan, U. Gorres, Z. Metallkd. 77 (1986) 43.
[38] D. Arias, J.P. Abriata, Bull. Alloy Phase Diagrams 11 (1990) 452.
[39] M.H. Braga, L.F. Malheiros, F. Castro, D. Soares, Z. Metallkd. 89 (1998) 541.
[40] K.P. Gupta, J. Phase Equil. 21 (2000) 553.
[41] H. Okamoto, J. Phase Equilib. Diff. 29 (2008) 204.
[42] K. Yamaguchi, Y.C. Song, T. Yoshida, K. Itagaki, J. Alloys Comp. 452 (2008) 73.
[43] O.J. Kleppa, S. Watanabe, Metall. Mater. Trans. B. 13B (1982) 391.
[44] F. Sommer, D.K. Choi, Z. Metallkd. 80 (1989) 263.
[45] M.A. Turchanin, I.V. Nikolaenko, J. Alloys Comp. 236 (1996) 236.
[46] A.I. Zaitsev, N.E. Zaitseva, High Temp. 41 (2003) 42.
[47] W. Gierlotka, K.C. Zhang, Y.P. Chang, J. Alloys Comp. 509 (2011) 8213.
[48] N. Saunders, Calphad 9 (1985) 297.
[49] K.J. Zeng, M. Hamalainen, H.L. Lukas, J. Phase Equilib. 15 (1994) 577.
[50] A.I. Zaitsev, N.E. Zaitseva, J.P. Alexeeva, S.F. Dunaev, Y.S. Nechaev, Phys. Chem. Chem. Phys. 5 (2003) 4185.
[51] N. Wang, C.R. Li, Z.M. Du, F.M. Wang, W.J. Zhang, Calphad 30 (2006) 461.
[52] G. Ghosh, Acta Mater. 55 (2007) 3347.
[53] S.H. Zhou, R.E. Napolitano, Acta Mater. 58 (2010) 2186.
[54] S.X. Cui, X.G. Xiso, H.Q. Hu, Z.T. Lv, G.Q. Zhang, Z.Z. Gong, Physica B 406 (2011) 3389.
[55] G. Kresse, M. Marsman, J. Furthüller, VASP the guide, http://cms.mpi.Univie.ac.at/vasp/.
[56] M.C. Payne, M.P. Teter, D.C. Allan, T.A. Arias, J.D. Joannopoulous, Rev. Mod. Phys. 64 (1992) 1045.
[57] P.E. Blöchl, Phys. Rev. B 50 (1994) 17953.
[58] P. Villars, L.D. Calvert, Pearson's handbook of crystallographic data for intermetallic phases [M], ASM International, Materials Park (OH), 1997.
[59] L. Vegard, Z. Phys 5 (1921) 17;
L. Vegard, Z. Kristallogr 67 (1928) 239.
[60] A.R. Denton, N.W. Ashcroft, Phys. Rev. A 43 (1991) 3161.
[61] B. Wen, T.J. Shao, R. Melnik, Y. Kawazoe, Y.J. Tian, J. Appl. Phys. 113 (2013) 103501.
[62] T.J. Shao, B. Wen, R. Melnik, S. Yao, Y. Kawazoe, J. Appl. Phys. 111 (2012) 083525.
[63] J.J. Zhao, J.M. Winey, Y.M. Gupta, Phys. Rev. B 75 (2007) 094105.
[64] B.M. Catti, Acta Crystallogr. Sect. A41 (1985) 494.
[65] C. Bercegeay, S. Bernard, Phys. Rev. B 72 (2005) 214101.
[66] W.C. Overton Jr., J. Gaffney, J. Phys. Rev. 98 (1955) 969.
[67] Z.J. Wu, E.J. Zhao, H.P. Xiang, X.F. Hao, X.J. Liu, J. Meng, Phys. Rev. B 76 (2007) 054115.
[68] O.L. Anderson, J. Phys. Chem. Solids 24 (1963) 909.
[69] D.H. Chung, W.R. Buessem, J. Appl. Phys. 39 (1968) 2777.
[70] J. Haines, J.M. Leger, G. Bocquillon, Annu. Rev. Mater. Res. 31 (2001) 1.
[71] B. Tsuchiya, R. Sahara, M. Oku, K. Konashi, S. Nagata, T. Shikama, H. Mizuseki, Y. Kawazoe, J. Alloys Comp. 489 (2) (2010) 685.
[72] R. Sahara, T. Shishido, A. Nomura, K. Kudou, S. Okada, V. Kumar, K. Nakajima, Y. Kawazoe, Phys. Rev. B 76 (2007) 0241051.
[73] S.F. Pugh, The Philos. Mag. 45 (1954) 823.
[74] K. Chen, L.R. Zhao, J. Rodgers, J.S. Tse, J. Phys. D: Appl. Phys. 36 (2003) 2725.
[75] D.G. Sangiovanni, V. Chirita, L. Hultman, Phys. Rev. B 81 (2010) 104107.
[76] Y. Wu, W. Hu, Eur. Phys. J. B 60 (2007) 75.
[77] S. Pauly, Acta Mater. 57 (2009) 5445.
[78] S.X. Cui, X.G. Xiao, H.Q. Hu, Z.T. Lv, G.Q. Zhang, Z.Z. Gong, Physica B 406 (2011) 3389.
[79] G.N. Greaves, A.L. Greer, R.S. Lakes, T. Rouxel, Nature Materials 10 (2011) 823.
[80] H.U. Kunzi, Top. Appl. Phys. 53 (1983) 169.
[81] C.A. Schuh, T.C. Hufnagel, U. Ramamurty, Acta Mater. 55 (2007) 4067.
[82] L. Fast, J.M. Wills, B. Johansson, O. Eriksson, Phys. Rev. B 51 (1995) 17431.
[83] E.M. Carvalho, I.R. Harris, J. Mater. Sci. 15 (1980) 1224.
[84] G. Ghosh, M. Asta, Acta Mater. 53 (2005) 3225.